



ELSEVIER

Journal of Alloys and Compounds 239 (1996) 193–197

Journal of
ALLOYS
AND COMPOUNDS

Metallurgical state of lanthanum and its effects on the activation behaviour of $Zr(Cr_{0.4}Ni_{0.6})_2$ hydride formation

Dalin Sun, J.M. Joubert, M. Latroche, A. Percheron-Guégan*

Laboratoire de Chimie Métallurgique et de Spectroscopie des Terres Rares, CNRS, 1 Place A. Briand, 92195 Meudon Cedex, France

Received 8 February 1996

Abstract

Lanthanum was added to cubic C15 type $Zr(Cr_{0.4}Ni_{0.6})_2$ to prepare $Zr(Cr_{0.4}Ni_{0.6})_2La_{0.05}$. Metallographical observation and microprobe analysis indicate that lanthanum does not dissolve in the Laves phase, but preferentially combines with nickel to form the LaNi phase which precipitates dispersively at the grain boundaries of the Laves phase together with Zr_7Ni_{10} . It is found by X-ray diffraction that the cell parameters of the Laves phase before and after adding lanthanum are the same. However, $Zr(Cr_{0.4}Ni_{0.6})_2La_{0.05}$ shows much better activation behaviour than $Zr(Cr_{0.4}Ni_{0.6})_2$, both in solid- H_2 reaction and alkaline electrolyte, which is believed to result from the presence of the LaNi phase.

Keywords: Lanthanum; Activation behaviour; Zr-based Laves phase; Hydride

1. Introduction

Zr-based Laves phase alloys are among the most promising materials for hydrogen energy applications, such as hydrogen storage, heat pumps and metal hydride batteries. However, in electrochemical applications they show a very poor activation behaviour in alkaline electrolyte if exposure to air occurs during the preparation of electrodes [1–3]. The reason for this has been attributed to the oxidation of elements and the formation of dense oxide layers on the surface of the powder, which prohibits the diffusion of hydrogen atom into the bulk. Therefore, many preliminary charge–discharge cycles are needed for activation. On the contrary, Sawa et al. [4] reported that the activation of Zr–Ti–V alloy electrodes was improved by an oxidation treatment, namely by annealing the electrode under low oxygen pressure (20–100 mmHg) at a temperature of 250–300°C. Furthermore, by means of X-ray photoelectron spectroscopy (XPS), Wang et al. [2] observed that such treatment resulted in the segregation of zirconium and titanium on the surface, while metallic nickel and vanadium precipitated in the

subsurface. This Ni-rich subsurface probably acts as an electrocatalyst and makes activation easier. From the above results, we believe that the activation behaviour of Zr-based Laves phase alloys is predominantly determined by the nature of their surface. Besides oxidation treatment, other surface treatments such as anodic treatment [1] and immersion in KOH or HF solution [3] were also found to modify the activation of Zr-based Laves phase alloy electrodes.

Recently, following the easy activation of La-based electrodes, Lee and coworker [5] observed that the activation of ZrCrNi electrode was greatly improved by adding light rare earth elements. It is well known that Laves phase often adopt two types of structure the hexagonal C14 ($MgZn_2$) type or the cubic C15 ($MgCu_2$) type. In the case of ZrCrNi the Laves phase exists as hexagonal C14 structure, but whether the addition of lanthanum would have the same positive effect on the Zr-based Laves phase alloy with cubic C15 structure is still unknown. Moreover, the metallurgical state of lanthanum in the Zr–Cr–Ni system has not been clearly identified so far.

In the present work, the metallurgical state of lanthanum in $Zr(Cr_{0.4}Ni_{0.6})_2$ is examined, and its effects on the activation behaviour investigated in solid- H_2 reaction as well as in alkaline electrolyte.

* Corresponding author.

2. Experimental procedures

2.1. Preparation of alloys

Zr(Cr_{0.4}Ni_{0.6})₂ with cubic C15 Laves phase was chosen as the parent alloy due to its well known hydrogenation properties from previous studies [6,7], and a small quantity of lanthanum was added to prepare Zr(Cr_{0.4}Ni_{0.6})₂La_{0.05}. These two alloys were synthesized from component elements with 99.9% purity by induction-melting in a water cooled copper crucible under argon atmosphere. Each sample was remelted five times to ensure homogeneity without any further heat treatment.

The metallurgical states were checked by metallographical observation and microprobe analysis. X-ray diffraction (XRD) experiments were performed on a Phillips PW1710 diffractometer using Cu K α radiation, and the diffraction patterns were refined to obtain structural parameters using the FULLPROF program [8] based on the Rietveld method.

2.2. Activation behaviour in solid-H₂ reaction

Samples were mechanically crushed into particles of less than 36 μm in air, and then put into hydrogenation reactors which were maintained at 25 °C throughout the experiments. After they had been outgassed, hydrogen was introduced into the reactors up to a pressure of 20 bar. The decrease in hydrogen pressure with time was recorded, and the absorbed hydrogen capacity of the alloy was subsequently calculated by the volumetric method. The relation between absorbed hydrogen capacity and time was used to compare the activation behaviour of Zr(Cr_{0.4}Ni_{0.6})₂ and Zr(Cr_{0.4}Ni_{0.6})₂La_{0.05} in solid-H₂ reaction. Subsequently the pressure-composition (*P-C*) isotherm was measured in the same apparatus.

2.3. Activation behaviour in alkaline electrolyte

The dependence of electrochemical capacity on charging-discharging cycles was determined in order to compare the effect of lanthanum on the activation of Zr(Cr_{0.4}Ni_{0.6})₂ in alkaline electrolyte. The electrodes were prepared by mixing the crushed samples with nickel powder and polytetrafluoroethylene in ammonia solution in a weight ratio of 25:70:5 and then cold pressed onto a nickel grid current collector. The electrochemical cell was built by sandwiching the metal hydride between two NiOOH/Ni(OH)₂ counter electrodes. The electrodes were galvanostatically charged at 40 mA g⁻¹, and then discharged at 50 mA g⁻¹ in a 6 M KOH solution at ambient temperature. The discharging cut-off potential was fixed at

-0.6 V with respect to a Hg/HgO, 6 M KOH reference electrode.

3. Results

3.1. Metallographical observation

Zr(Cr_{0.4}Ni_{0.6})₂La_{0.05} was found to easily form holes on the polishing surface (see Fig. 1); using the same procedures for preparing metallographical samples no hole was observed on the surface of Zr(Cr_{0.4}Ni_{0.6})₂. Fig. 1 also indicates that there is a second phase which precipitates dispersively in the matrix after addition of lanthanum. This second phase was subsequently identified by microprobe analysis as LaNi.

After etching with 3% HF solution, both Zr(Cr_{0.4}Ni_{0.6})₂ and Zr(Cr_{0.4}Ni_{0.6})₂La_{0.05} showed the same metallographical features, see Figs. 2(a) and 2(b). The white areas in Figs. 2(a) and 2(b) belong to the Laves phase, and the black one which distributes between the grain boundaries of the Laves phase is attributed to the second phase.

3.2. Microprobe analysis and XRD

Microprobe analysis and XRD were employed to determine the metallurgical phases and their cell parameters in Zr(Cr_{0.4}Ni_{0.6})₂ and Zr(Cr_{0.4}Ni_{0.6})₂La_{0.05}.

For both alloys, microprobe analysis shows that the major phase is the Laves phase with a few of chromium segregation in its centre. The second phase which corresponds to the black area in Fig. 2(a) is Zr₇Ni₁₀, as already reported in Ref. [6]. However, comparing with Zr(Cr_{0.4}Ni_{0.6})₂, the black area of

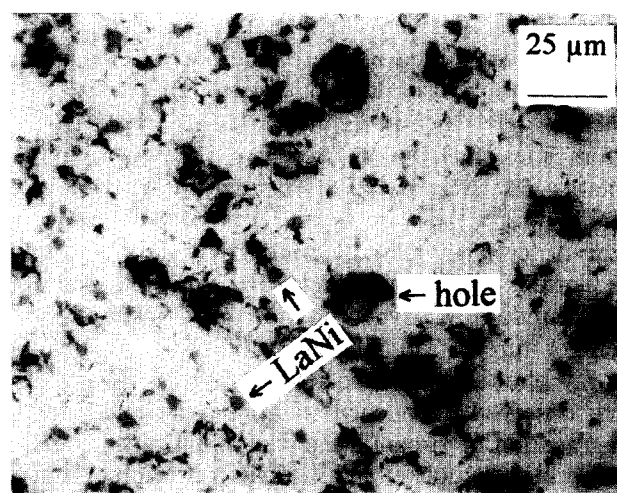


Fig. 1. Metallographic photograph of Zr(Cr_{0.4}Ni_{0.6})₂La_{0.05}, no etching.

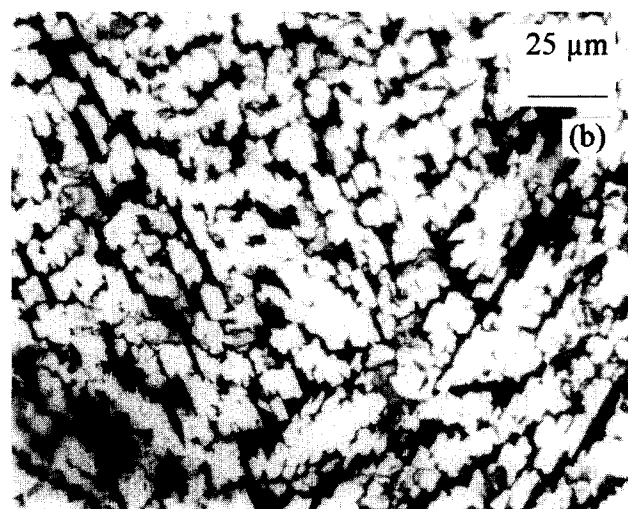
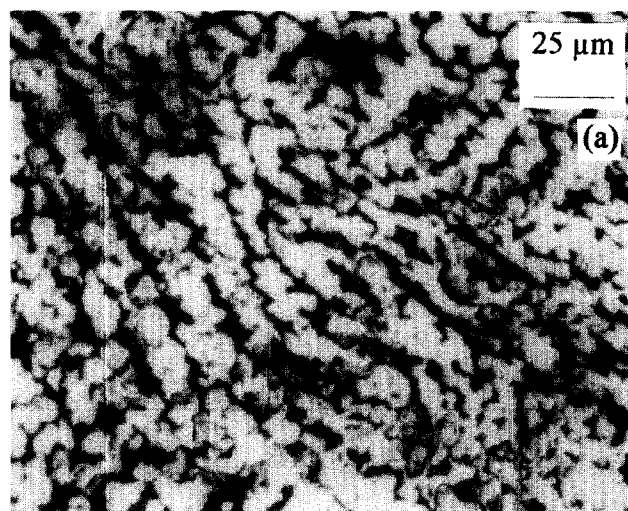


Fig. 2. Metallographic features after etching: (a) $Zr(Cr_{0.4}Ni_{0.6})_2$, (b) $Zr(Cr_{0.4}Ni_{0.6})_2La_{0.05}$.

$Zr(Cr_{0.4}Ni_{0.6})_2La_{0.05}$ in Fig. 2(b) is Zr_7Ni_{10} and $LaNi$. Moreover, XRD reveals that the Laves phase of the two alloys has the cubic C15 structure. These final results are summarized in Tables 1 and 2.

Table 1
Characteristics of $Zr(Cr_{0.4}Ni_{0.6})_2$

Phase	Average composition (at.%)			Structure type	Cell parameters (Å)
	Zr	Cr	Ni		
Laves phase	30.5(4.0)	40.1(6.1)	29.4(3.8)	Cubic C15	$a = 7.059(1)$
Zr_7Ni_{10}	40.2(2.8)	3.6(1.1)	56.2(1.3)	Orthorhombic	$a = 9.212(1)$ $b = 9.175(1)$ $c = 12.353(2)$
Cr ^a	1.2(0.9)	96.2(2.0)	2.6(1.3)	—	—

^a No diffraction peak appears in XRD pattern due to its limited quantity.

It is interesting to note that Tables 1 and 2 that lanthanum does not dissolve into the Laves phase, and the cell parameters of the Laves phase in the two alloys are the same.

3.3. Activation behaviour in solid- H_2 reaction

The relation between the absorbed hydrogen capacity and time in the solid- H_2 reaction for $Zr(Cr_{0.4}Ni_{0.6})_2$ and $Zr(Cr_{0.4}Ni_{0.6})_2La_{0.05}$ is shown in Fig. 3. It indicates that $Zr(Cr_{0.4}Ni_{0.6})_2$ does not absorb hydrogen when the reaction time is less than 6 h, and takes about 88 h to be well activated; while $Zr(Cr_{0.4}Ni_{0.6})_2La_{0.05}$ takes only about 0.66 h (40 min) to appreciably absorb hydrogen under the same conditions. Therefore it can be concluded that hydrogen absorption is greatly enhanced by the addition of lanthanum to cubic $Zr(Cr_{0.4}Ni_{0.6})_2$.

3.4. Comparison of P-C isotherms

The hydrogen absorption isotherms before and after addition of lanthanum at 25 °C are compared in Fig. 4. It shows that the two curves exhibit a similar tendency with no significant difference, and the maximum capacities at 10 bar are almost the same. In Fig. 4 the curve of $Zr(Cr_{0.4}Ni_{0.6})_2$ taken from our previous work [7] indicates a slightly higher pressure than that of $Zr(Cr_{0.4}Ni_{0.6})_2La_{0.05}$, which may be caused by the higher nickel content (39.1(7) at.%) in the Laves phase due to annealing at 1000 °C for one month.

3.5. Activation behaviour in alkaline electrolyte

The dependence of discharge capacities on charging-discharging cycles is shown in Fig. 5. It can be seen that the discharge capacity of $Zr(Cr_{0.4}Ni_{0.6})_2$ increases slowly with the increment of cycles, and the discharge capacity is less than 100 mA h g⁻¹ even after 10 cycles. However, the initial discharge capacity of $Zr(Cr_{0.4}Ni_{0.6})_2La_{0.05}$ reaches 230 mA h g⁻¹, which is

Table 2
Characteristics of $\text{Zr}(\text{Cr}_{0.4}\text{Ni}_{0.6})_2\text{La}_{0.05}$

Phase	Average composition (at.%)				Structure type	Cell parameters (Å)
	Zr	Cr	Ni	La		
Laves phase	31.5(4.7)	36.3(7.2)	32.2(6.7)	0.0(0.1)	Cubic C15	$a = 7.058(1)$
$\text{Zr}_7\text{Ni}_{10}$	38.6(2.2)	4.0(1.6)	55.1(1.3)	2.3(0.4)	Orthorhombic	$a = 9.220(8)$ $b = 9.206(8)$ $c = 12.318(7)$
LaNi^a	4.4(0.8)	2.0(0.8)	47.4(3.6)	48.3(4.2)	—	—
Cr^a	0.0(0.1)	99.3(0.2)	0.7(0.6)	0.0(0.1)	—	—

^a No diffraction peak appears in XRD pattern due to its limited quantity.

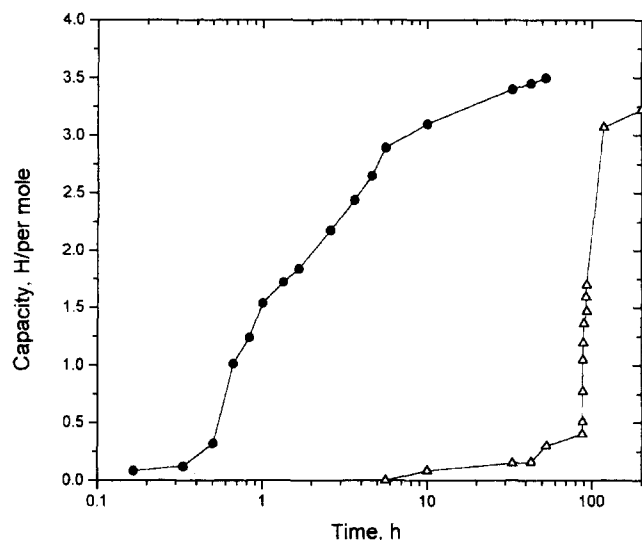


Fig. 3. The relation between absorbed hydrogen capacity and time: Δ , $\text{Zr}(\text{Cr}_{0.4}\text{Ni}_{0.6})_2$; \bullet , $\text{Zr}(\text{Cr}_{0.4}\text{Ni}_{0.6})_2\text{La}_{0.05}$.

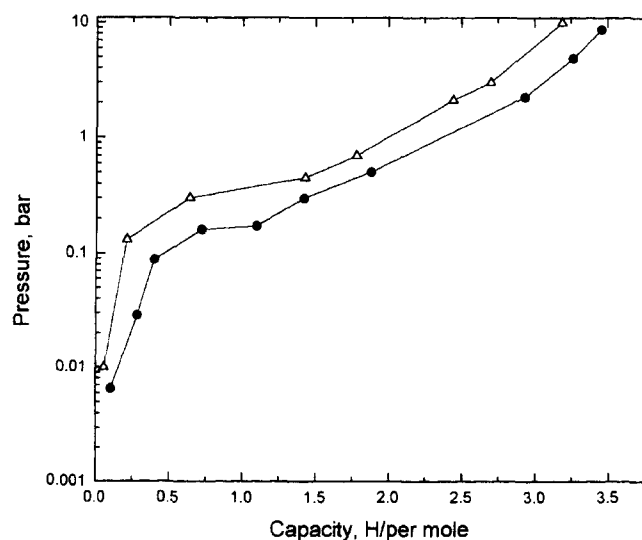


Fig. 4. P - C curves before and after addition of lanthanum at 25°C: Δ , $\text{Zr}(\text{Cr}_{0.4}\text{Ni}_{0.6})_2$ [8]; \bullet , $\text{Zr}(\text{Cr}_{0.4}\text{Ni}_{0.6})_2\text{La}_{0.05}$.

nearly close to the measured maximum value; that is, no need of preliminary charging–discharging cycles for its activation.

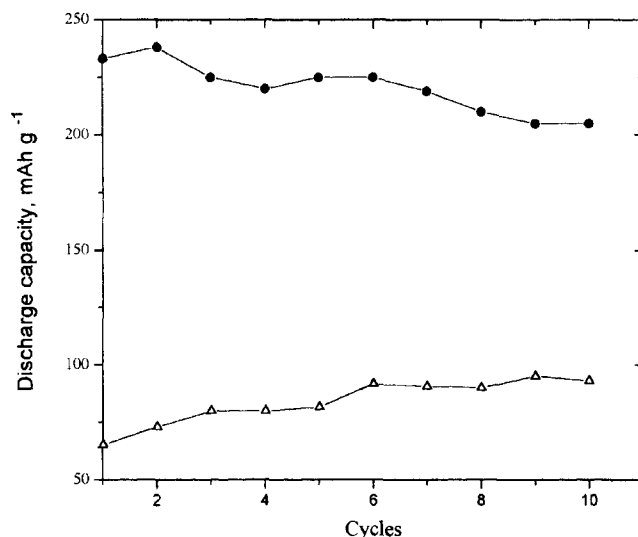


Fig. 5. Dependence of discharge capacities on charging–discharging cycles: Δ , $\text{Zr}(\text{Cr}_{0.4}\text{Ni}_{0.6})_2$; \bullet , $\text{Zr}(\text{Cr}_{0.4}\text{Ni}_{0.6})_2\text{La}_{0.05}$.

4. Discussion

After etching with 3% HF solution, both $\text{Zr}(\text{Cr}_{0.4}\text{Ni}_{0.6})_2$ and $\text{Zr}(\text{Cr}_{0.4}\text{Ni}_{0.6})_2\text{La}_{0.05}$ show similar metallographical features, as shown in Fig. 2. Microprobe analysis and XRD reveal that the major phase in the two alloys is the cubic C15 Laves phase, and some chromium segregating in the centre of the Laves phase possibly occurs during cooling from melting. The second phase which is distributed between the grain boundaries of the Laves phase is $\text{Zr}_7\text{Ni}_{10}$; but comparing with $\text{Zr}(\text{Cr}_{0.4}\text{Ni}_{0.6})_2$, a new additional phase, LaNi , appears with $\text{Zr}_7\text{Ni}_{10}$ in $\text{Zr}(\text{Cr}_{0.4}\text{Ni}_{0.6})_2\text{La}_{0.05}$. Because lanthanum does not dissolve into the Laves phase as shown in Table 2, it does not change the cell parameters of the Laves phase, which is in agreement with the refined data from XRD using the FULLPROF program.

The poorer activation of $\text{Zr}(\text{Cr}_{0.4}\text{Ni}_{0.6})_2$ shown in solid- H_2 reaction and alkaline electrolyte can reasonably be attributed to the oxidation of zirconium, chromium and the surface oxide layers formed in air [9,10]. However, $\text{Zr}(\text{Cr}_{0.4}\text{Ni}_{0.6})_2\text{La}_{0.05}$ shows much better activation behaviour than $\text{Zr}(\text{Cr}_{0.4}\text{Ni}_{0.6})_2$. Al-

though Zr_7Ni_{10} was also reported to have a good electrocatalytic effect on the activation of Zr-based Laves phase alloys [7], this positive effect is not observed in the present study of $Zr(Cr_{0.4}Ni_{0.6})_2$ because there is not sufficient Zr_7Ni_{10} present as the second phase, see Fig. 5. Therefore, the addition of lanthanum to $Zr(Cr_{0.4}Ni_{0.6})_2$ with cubic C15 Laves phase is believed to improve the activation behaviour in the alkaline electrolyte, just as in the case of ZrCrNi with hexagonal C14 Laves phase structure [5]. Considering the results of microprobe analysis, we are sure that this improvement results from the appearance of the LaNi phase after addition of lanthanum. This is because not only can LaNi readily absorb large amounts of hydrogen at room temperature [11], but lanthanum oxide formed in air would also make the activation process easier [9]. Therefore, the existence of LaNi as a second phase in $Zr(Cr_{0.4}Ni_{0.6})_2La_{0.05}$ may be regarded as “active sites”, which allow hydrogen atoms to penetrate easily through the oxide layers and make the activation of the alloy faster. This is probably the reason for the different activation behaviour shown by $Zr(Cr_{0.4}Ni_{0.6})_2$ and $Zr(Cr_{0.4}Ni_{0.6})_2La_{0.05}$.

5. Conclusions

Within the range of present study it is found that lanthanum does not dissolve into the Laves phase of $Zr(Cr_{0.4}Ni_{0.6})_2$ but will preferentially combine with nickel to form LaNi which precipitates dispersively between the grain boundaries of the Laves phase together with Zr_7Ni_{10} . Owing to the zero solubility of lanthanum, the cell parameters of the Laves phase in $Zr(Cr_{0.4}Ni_{0.6})_2$ and $Zr(Cr_{0.4}Ni_{0.6})_2La_{0.05}$ are the same.

In comparison, $Zr(Cr_{0.4}Ni_{0.6})_2La_{0.05}$ shows much better activation behaviour than $Zr(Cr_{0.4}Ni_{0.6})_2$, both in solid- H_2 reactions and in alkaline electrolyte. This is believed to result from the presence of the LaNi phase after addition of lanthanum. In addition, our further experiments have confirmed the same positive effect of lanthanum on other kinds of Zr-based Laves phase alloy with cubic C15 structure. Therefore it can be concluded that the addition of lanthanum will improve the activation behaviour of Zr-based Laves phase alloys with cubic C15 structure.

References

- [1] S. Wakao, H. Sawa and J. Furukawa, *J. Less-Common Met.*, 172–174 (1991) 1219.
- [2] X. Wang, S. Suda and S. Wakao, *Z. Phys. Chem.*, 183 (1994) 297.
- [3] A. Züttel, F. Meli and L. Schlapbach, *J. Alloys Comp.*, 209 (1994) 99.
- [4] H. Sawa, M. Ohta, H. Nakano and S. Wakao, *Z. Phys. Chem., N.F.*, 164 (1989) 1527.
- [5] S.R. Kim and J.Y. Lee, *J. Alloys Comp.*, 185 (1992) L1.
- [6] J.M. Joubert, M. Latroche, I. Ansara and A. Percheron-Guégan, *J. Phase Equilib.* 16 (1995) 485.
- [7] J.M. Joubert, M. Latroche, A. Percheron-Guégan and J. Bouet, *J. Alloys Comp.*, in press.
- [8] J. Rodriguez-Carjaval, *Abstr. Satellite Meet. on Powder Diffraction, Congr. Int. Union of Crystallography, Toulouse, France, 1990*, p. 127.
- [9] S.R. Kim, J.Y. Lee and H.H. Park, *J. Alloys Comp.*, 205 (1994) 225.
- [10] A. Züttel, F. Meli and L. Schlapbach, *Z. Phys. Chem.*, 183 (1994) 355.
- [11] K.H.J. Buschow, P.C.P. Bouten and A.R. Miedema, *Rep. Progr. Phys.*, 4 (1982) 937.